Science of the Total Environment 665 (2019) 502–512

Contents lists available at ScienceDirect

Science of the Total Environment

journal homepage: www.elsevier.com/locate/scitotenv

Lead, zinc, and copper redistributions in soils along a deposition gradient from emissions of a Pb-Ag smelter decommissioned 100 years ago

R. Gelly [a,*], Z. Fekiacova [a], A. Guihou [a], E. Doelsch [b], P. Deschamps [a], C. Keller [a]

[a] Aix Marseille Univ., CNRS, IRD, INRA, Coll France, CEREGE, Technopôle de l'Environnement Arbois-Méditerranée, BP 80, F-13545 Aix-en-Provence, France
[b] CIRAD, UPR Recyclage et risque, F-34398 Montpellier, France Recyclage et Risque, Univ Montpellier, CIRAD, Montpellier, France

HIGHLIGHTS

- Pb isotopes, δZn, δCu in soils impacted by emissions from a smelter 100 y ago.
- Pb contamination was detected 7 km away from the smelter and down the soil profiles.
- Light δ^{66}Zn values were measured in the chimney and in soil surface horizons.
- Precipitation of Zn-Layered Double Hydroxide prevented downward migration of anthropogenic Zn.
- Cu isotopes indicate its geogenic origin and redistribution in soils by pedogenesis.

GRAPHICAL ABSTRACT

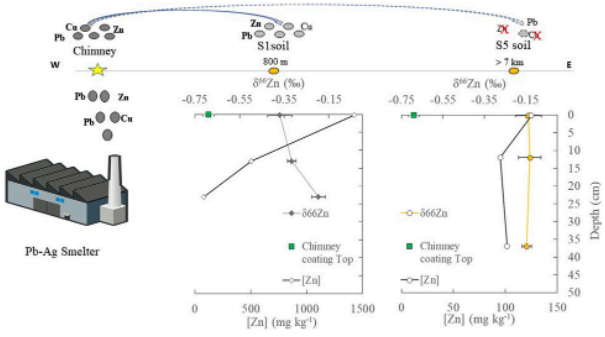

ARTICLE INFO

Article history:
Received 13 November 2018
Received in revised form 5 February 2019
Accepted 5 February 2019
Available online 08 February 2019

Editor: Mae Sexauer Gustin

Keywords:
Metal contamination
Stable isotopes
Historical contamination
Metal cycling
Smelting

ABSTRACT

Sourcing and understanding the fate of anthropogenic metals in a historical contamination context is challenging. Here we combined elemental and isotopic (Pb, Zn, Cu) analyses with X-ray Absorption Spectroscopy (XAS) measurements (Zn) to trace the fate, in undisturbed soil profiles, of historical metal contamination emitted by a 167-year-old Pb-Ag smelter decommissioned 100 years ago located in the Calanques National Park (Marseilles, France). Lead isotopic measurements show that entire soil profiles were affected by 74 years of Pb emissions up to ~7 km from the smelter under the main NNW wind, and indicate particulate transfer down to 0.8 m at depth. This vertical mobility of anthropogenic Pb contrasts with previous studies where Pb was immobilized in surface horizons. The contribution of anthropogenic Pb to the total Pb concentration in soil was estimated at 95% in surface horizons, and 78% in the deepest horizons. Zinc isotopic signatures of past emissions that are enriched in light isotopes compared to the natural geological background (-0.70 ± 0.04‰ and -0.15 ± 0.02‰, respectively), were detected only in the surface horizons of the studied soils. Using XAS analyses, we showed that anthropogenic Zn was transformed and immobilized in surface horizons as Zn-Layered Double Hydroxide, thus favoring the enrichment in heavy isotopes in these surface horizons. No clear evidence of copper contamination by the smelter was found and Cu isotopes point to a bedrock origin and a natural distribution of Cu concentrations.

© 2019 Elsevier B.V. All rights reserved.

1. Introduction

Lead (Pb), zinc (Zn) and copper (Cu) are trace elements naturally present in soils at concentrations usually below 1000 mg kg^{-1} (Kabata-

* Corresponding author.
E-mail address: gelly@cerege.fr (R. Gelly).

https://doi.org/10.1016/j.scitotenv.2019.02.092
0048-9697/© 2019 Elsevier B.V. All rights reserved.

Pendias, 2011). They are also released by human activities through emission to the atmosphere or direct application (e.g. by smelting, fossil energy consumption and soil fertilization). Lead is toxic to living organisms even at low doses (World Health Organization et al., 1996). Zinc and Cu are micro-nutrients required in biochemical reactions, but their excessive concentrations lead to toxicity (World Health Organization et al., 1996). In soils, distinguishing between the natural and anthropogenic origins of Pb, Zn and Cu is still a challenge as pedogenetic processes redistribute metals within soil profiles and alter their speciation (Legros, 2007; Semlali et al., 2001). Yet, the distinction is essential for tracing the source of contamination and transfer in soils, and for identifying the potential risks of increased anthropogenic metal transfer in the environment and associated remediation plans.

Since the 1990s, Pb isotopes have proved to be powerful tracers of Pb contamination related to gasoline emissions (Erel et al., 1997; Luck and Ben Othman, 2002; von Storch et al., 2003) and to emissions from industrial areas (Cloquet et al., 2006; Jeon et al., 2017; Wen et al., 2015). Furthermore, Pb isotopes have been used for tracing the transport and redistribution of Pb in the atmosphere (Desenfant et al., 2006; Hamelin et al., 1997; Shotyk et al., 2002; Véron et al., 1999; Weiss et al., 2002). More recently, Cu and Zn isotopes were used to link increased metal concentrations in soils or sediments to the emissions of metallurgic plants (Araújo et al., 2018; Bigalke et al., 2010; Juillot et al., 2011; Kříbek et al., 2018; Mihaljevič et al., 2018; Sivry et al., 2008; Sonke et al., 2008; Thapalia et al., 2010), or for sourcing metal particles from mining and tailing sites (Borrok et al., 2009; Kimball et al., 2009; Song et al., 2016; Viers et al., 2018). Anthropogenic Cu and Zn isotope tracing relies on large isotopic fractionation (Mattielli et al., 2009; Ochoa Gonzalez and Weiss, 2015; Shiel et al., 2010; Wiederhold, 2015) created during high-temperature industrial processes (e.g., smelting) generating particles emitted to the atmosphere that are enriched in light isotopes and distinct from the isotopic signatures of soil and from any potential small isotopic fraction induced by natural effects.

Most of the above-mentioned studies were conducted on soils near active Zn or Cu smelters with ongoing emissions and only a few focused on long-abandoned contaminated sites (Juillot et al., 2011; Sivry et al., 2008; Sonke et al., 2008). Understanding the fate of historical contamination is challenging because it requires considering the effect of pedogenesis on metal cycling. It has been shown that pedogenetic processes alter Zn and Cu isotopic signatures through post-deposition fractionation (Juillot et al., 2011; Šillerová et al., 2017; Weiss et al., 2008) that with time, may compromise the identification of metal-sources. This post-deposition fractionation is caused by plant uptake of Zn and Cu depleting the soil in light isotopes (Aucour et al., 2015; Jouvin et al., 2012; Viers et al., 2007; Weinstein et al., 2011) and by metal-sorption to soil particles such as Fe-Mn oxides (Balistrieri et al., 2008; Bigalke et al., 2011; Bryan et al., 2015; Juillot et al., 2008; Pokrovsky et al., 2005, 2008) or organic matter (Jouvin et al., 2009; Opfergelt et al., 2017) favoring heavy isotope enrichments in soils.

In the 19th century, The Marseilleveyre Massif (Marseilles, France) was home to numerous heavy industries that have left derelict sites. While the area is now enclosed in the Calanques National Park and is highly protected, it was found to be extensively impacted by these activities (Daumalin and Raveux, 2016). The site of a former Pb-Ag smelter, located in the Escalette Calanque, west of the massif, is particularly appropriate for studying the fate of a historical metal contamination (Figs. 1 and S1). It processed argentiferous galena ores from 1851 to 1925 by pyrometallurgical processes and generated massive dumps of Pb and Zn-rich slags and atmospheric emissions of highly metal-concentrated particles. Previous investigations (Affholder et al., 2013; Testiati et al., 2013) showed that soil metal and metalloid concentrations (i.e. Pb, Sb, Zn, Cd and Cu) in the immediate vicinity of the smelter are well above the values of the local biogeochemical background (Austruy et al., 2016). However, no further investigations were performed to evaluate the anthropogenic origin of the metals in more distant soils, or to identify a possible vertical contamination along the soil profile.

In this study we combined elemental and isotopic Pb, Zn and Cu measurements with X-ray Absorption Spectroscopy (XAS for Zn) analyses to: (i) characterize the isotopic signatures of the pollution originating from the historical Escalette smelter; (ii) determine whether the Cu concentrations in soils result from galena ore processing or represent natural occurrences; (iii) assess the extent of the vertical transfer of the contamination in a selection of soils of the Calanques National Park located along a transect of increasing distance from the smelter.

The Escalette smelter did not process Cu. However, significant amounts of Cu can be present in galena ores, as Cu can substitute into the crystal lattice (George et al., 2015). Thus, we decided to use Cu isotopes to investigate whether traces of anthropogenic Cu could have been generated during the smelting of galena and whether they could be detected in the surrounding soils.

Coupling Zn and Cu isotopes with Pb isotopes that are not affected by isotopic fractionation in soils could help clarify the source of Zn and Cu if the signatures of these elements are too compromised; this is especially the case in subsurface horizons where the pedogenetic processes are the most effective. Furthermore, combining Zn isotopic signatures with Zn-speciation in soils by XAS measurements could shed light on the possible alteration of Zn by pedogenetic processes and/or on the transformation of Zn-bearing phases in soils. This method has proved to be efficient for investigating the cycling of anthropogenic Zn in a soil-plant system (Aucour et al., 2015; Juillot et al., 2011). Such a combination of analytical tools with multi-isotope systems was proposed by Wiederhold (2015). To our knowledge, a combination of Pb, Zn and Cu isotopes has been attempted in only one study dedicated to sourcing of urban aerosols (Souto-Oliveira et al., 2018), and it has never been used for soil studies nor in combination with XAS measurements.

2. Material and methods

2.1. Smelter samples

The Escalette smelter produced PbO and $Ag_{(s)}$ by roasting PbS ores before casting under oxidic conditions at ~1100 °C, and separation of Pb and Ag. A detailed description of the pyrometallurgical process can be found in Carlier et al. (2010). We collected eight slags resulting from the smelting process along a solid reddish deposit located behind the smelter (Fig. S1, Table S1d).

Grey coatings that had accumulated on the walls of the remaining creeping chimney (ca 300 m-long) were sampled at both ends (i.e. close to the furnace and close to the exit) and in shielded parts not exposed to external climatic conditions. Sampling of true emitted particles was impossible since the smelter has been decommissioned. Considering that the chimney was not equipped with any kind of particle-filtering system, we postulated that the chemical and isotopic compositions of the sample collected at the top end of the chimney were the closest to those of the metals emitted into the atmosphere and to those deposited onto the soils of the surrounding area. Thus, it can be used as a proxy for the material deposited at the surface of the soils in the vicinity of the smelter.

2.2. Soil samples

We selected five soil profiles along a 7-km NW-SE transect (Figs. 1 and S1) of increasing distance from the former smelter, and downwind of the dominant and most powerful wind (NW-SE). These soils were developed on a marine limestone parent material of Cretaceous age, with low metal concentrations (Text S1). The surrounding vegetation is typical of the Mediterranean area (Affholder et al., 2013; Testiati et al., 2013).

These five soil profiles (S1, S2, S3, S4 and S5), labeled in order of increasing distance from the smelter, were sampled and described

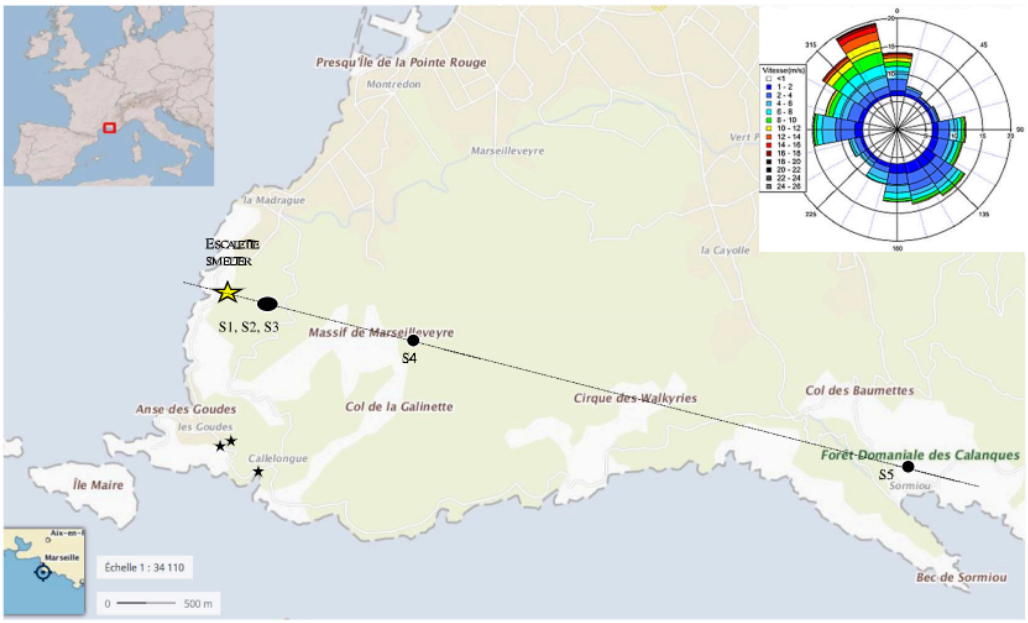

Fig. 1. Global Marseilleveyre Massif map near Marseilles (France). Average wind directions over 10 years (2001−2011) obtained from Marignane station (METEOFRANCE data). Dotted line indicates the 7 km NW-SE studied transect with relative position of the soil profiles under the main wind NNW from the Escalette smelter (yellow star) to S5 soil (black dot). Black stars highlight the position of other industries (Pb smelter (1854–1878), soda-production factory (1854–1894), sulfur refinery (1860–1900) operating at the beginning of the Escalette smelter exploitation (1851–1925). (For interpretation of the references to color in this figure legend, the reader is referred to the web version of this article.)

according to the soil horizons. They were selected because of their similar morphological and physico-chemical characteristics to ensure that different soil properties and/or pedogenetic processes did not introduce any bias in the metal-distribution. They are Colluviosols (Baize et al., 2009) or Leptosols (colluvic) (FAO, 2006) with a near neutral pH of 8, an average organic carbon content of 37.3 g kg^{-1} and a mean $CaCO_3$ content of 247 g kg^{-1}. All the profiles presented a loose and permeable stone/gravel layer of several centimeters resulting from colluvial movements and set above the usual organic litter and A horizon. X-Ray Diffraction results and physico-chemical characteristics of the samples, determined by the Laboratoire d'Analyse des Sols (LAS) at Arras (INRA, France) are available in SI (Tables S1a, b).

2.3. Total concentrations and isotopic analyses

Total concentrations and isotopic analyses were performed on the bulk soils, slags, and chimney coatings. All soil samples were air dried and sieved to <2 mm. They were further crushed to a fine powder in a mechanical agate mortar. For total metal concentrations and isotopic analyses, 150 mg of soil sample powder were weighed and calcined at 450 °C for 4 h to eliminate organic matter, then dissolved using a mixture of concentrated HNO_3-HF-HCl at 130 °C. Reagents were either distilled acids (HNO_3, HCl) or Seastar© quality (HF). Slags and chimney coatings were ground to a fine powder in an agate mortar and 50 mg of material was totally dissolved using 5 ml of *aqua regia* at 130 °C.

After digestion, total Pb, Zn and Cu concentrations were measured in solution using a PerkinElmer NexIon 300× Q-ICP-MS with ^{103}Rh as internal standard. Calibration curves were made by dilution of the standards (CCS4, CCS5 and CCS6 from Inorganic Ventures, New Jersey, USA) in HNO_3 2%. Quality control was ensured by measuring in each run the EnviroMAT EP-L-3, the EnviroMAT ES-H-2 (SCP Sciences Courtaboeuf, France), and the SRLS-5 (Ottawa, Canada) reference materials. Quantification limits were 0.003 µg l^{-1} for Pb, 0.005 µg l^{-1} for Cu, and 0.05 µg l^{-1} for Zn.

For isotopic analyses, Cu, Zn and Pb were separated and purified using ion exchange chromatography. Copper and Zn were separated and purified using an anionic resin (AG-MP1, 100–200 mesh, chloride form), following the procedure published in Maréchal et al. (1999). Lead was separated using an anionic resin (AG1-X8, 100–200 mesh) following the procedure published in (Fekiacova et al., 2007; Lugmair and Galer, 1992).

Measurements of Pb, Zn and Cu isotopic compositions were carried out at CEREGE using a Thermo Fisher Scientific Neptune^{Plus} Multi-Collector Inductively Coupled Plasma Mass Spectrometer (MC-ICP-MS). ^{208}Pb, ^{207}Pb, ^{206}Pb, ^{204}Pb isotopes corrected for instrumental blanks and mass bias fractionation were measured and are reported as isotope ratios for Pb and as δ notation (per-mil) for Zn (1) and Cu (2) relative to the IRMM-3702 Zn isotopic standard and the AES-633 Cu isotopic standard.

$$\delta^{66}Zn = \left(\frac{\left(\frac{66Zn}{64Zn}\right)Sample}{\left(\frac{66Zn}{64Zn}\right)IRMM3702} - 1 \right) * 1000 \quad (1)$$

$$\delta^{65}Cu = \left(\frac{\left(\frac{65Cu}{63Cu}\right)Sample}{\left(\frac{65Cu}{63Cu}\right)AES633} - 1 \right) * 1000 \quad (2)$$

All data cited in the present paper are expressed relative to the IRMM-3702 standard for Zn and to the AES-633 standard for Cu. In order to compare our data with data from the literature expressed versus the no longer commercially available JMC-37049L (Zn) and NIST-976 (Cu) standards, the following equations were used (Sossi et al., 2015).

$$\delta^{66}Zn_{IRMM3702} = \delta^{66}Zn_{JMC37049L} - 0.3 \pm 0.02‰$$

$$\delta^{65}Cu_{AES633} = \delta^{65}Cu_{NIST976} + 0.01 \pm 0.05‰$$

For δ^{66}Zn and δ^{65}Cu, three measurements of each sample digestion were made and expressed as the average value of the three measurements; their repeatability is expressed as two standard deviations (2SD). Seven samples (i.e. all surface horizons of the soils from S1 to S5 and the chimney coatings, top and bottom) were duplicated by conducting a second sample preparation (digestion, column separation and analyses). Reproducibility of the replicated analyses was determined using ANOVA and presented as 2SD. Accuracy was controlled by processing the USGS reference material NOD-P-1 (Manganese nodule) with each batch of samples and reproducibility was calculated on the basis of 6 full replicates using the ANOVA procedure (Addinsoft, 2016). This material is well characterized for Zn (0.55 ± 0.08‰; 0.48 ± 0.09‰) and Cu (0.36 ± 0.08‰; 0.47 ± 0.08 isotopic compositions (Bigalke et al., 2010; Chapman et al., 2006). The mean Zn (δ^{66}ZnIRMM-3702: 0.53 ± 0.08‰) and Cu (δ^{65}CuAES-633: 0.45 ± 0.08‰) isotopic compositions of NOD-P-1 obtained during this study agree with previously published data (Bigalke et al., 2010; Chapman et al., 2006). In addition to the Mn-nodule reference material, soil standards (e.g. GBW07402 from the National Research Centre of Geoanalysis, Beijing, China, TILL-1 from the CANMET Mining and Mineral Sciences Laboratories, Ottawa, Canada) were also processed during this study. Their δ^{66}ZnIRMM-3702 and δ^{65}CuAES-633 isotopic compositions were measured at 0.01 ± 0.07‰. However, these results could not be compared to the literature as no values have been published for these standards so far.

Copper and Zn chromatographic separation yields of processed samples were measured at 100% ± 10%. A further indicator of data quality is the strong correlation between δ^{66}Zn and δ^{67}Zn that matches mass-dependent fractionation processes as specified in (Maréchal et al., 1999) (Fig. S2).

For Pb isotopes, one measurement was carried out per sample digestion. The repeatability of analyses was estimated from multiple measurements of the bracketing standard NBS981 and is expressed as two standard deviations (2SD).

More information on the procedure can be found in SI (Text S2).

2.4. EXAFS spectra acquisition and analysis

Zinc K-edge X-ray absorption spectra were recorded on samples of the chimney coatings (top) and the surface horizons of S1 and S5 at the ESRF (Grenoble, France) on the BM30B (FAME) beamline. Spectra were measured at liquid helium temperature and in fluorescence mode with a 30-element solid state Ge detector. Normalization and data reduction were performed according to standard methods (Doelsch et al., 2006) using Athena software (Ravel and Newville, 2005). A library of Zn reference compound spectra, described elsewhere (Formentini et al., 2017; Legros et al., 2017) was used to identify Zn species in the samples. Details on the fitting procedure and results are given in SI (Text S3, Fig. S3a, b and Table S2).

3. Results and discussion

3.1. Characterization of slags and grey coatings originating from the former smelter

The Escalette smelter processed various sources of Pb-ores during its exploitation (Daumalin and Raveux, 2016). This variability of sources can impact the isotopic signatures of the volatile and residual phases formed during the smelter process. Moreover, high temperature processes are also known to induce large isotopic fractionation, particularly for Zn.

The Pb isotopic compositions of the sampled slags ranged from 2.0759 to 2.0999 and from 0.8371 to 0.8529, for $^{208}Pb/^{206}Pb$ and $^{207}Pb/^{206}Pb$ ratios, respectively (Table S1c). As Pb isotopes do not fractionate during the smelting of Pb-Zn ores (Cui and Wu, 2011; Shiel et al., 2010), this heterogeneity reflects the isotopic variability of the ores used during operation of the smelter (Daumalin and Raveux, 2016). By comparing historical reports of the smelter production and a published compilation of the Pb isotopic signature of the main ores (Stos-Gale et al., 1995), two Pb-Ag ores were identified as the origin of these slags: one from the Tuviois ore district (Sardinia, Italy) and the other from the Murcia Mazzaron district (Spain) that is consistent with the historical data found in (Daumalin and Raveux, 2016). The chimney recorded the isotopic signatures of all the processed ores, thus yielding an average Pb isotopic signature typical of the smelter emissions and characterized by values of 2.0924 and 0.8471, for $^{208}Pb/^{206}Pb$ and $^{207}Pb/^{206}Pb$, respectively (Table S1c).

Zinc and Cu isotopic compositions of slags and chimney coatings are presented in Fig. 3(b, c) and Tables S1(c, d). Zinc isotopic composition of the slags, ranged from −0.36 ± 0.01‰ to −0.14 ± 0.05‰ ($n = 8$), was heavier than that of the chimney coatings. Grey deposits collected in the chimney were enriched in light isotopes: −0.70 ± 0.04‰ (top sample used as a proxy for the emitted particles, close to the chimney exit) and −0.26 ± 0.09‰ (bottom, close to the furnace) that is consistent with previously published values for Zn or Cu smelters (Bigalke et al., 2010; Mattielli et al., 2009; Sonke et al., 2008).

Previous studies demonstrated the enrichment of dust particles in light Zn isotopes resulting from Rayleigh-type isotope fractionation (Bigalke et al., 2010; Mattielli et al., 2009; Shiel et al., 2010; Yin et al., 2016). This mechanism was also active during the Escalette smelting process and produced chimney deposits, enriched in light isotopes. Conversely, residual slags were enriched in heavy isotopes. Yet, the Rayleigh distillation did not produce slags with the same δ^{66}Zn value as we measured slight variations in the δ^{66}Zn values of these samples. These variations could reflect the isotopic variability of the galena ores used throughout 74 years of activity. This has also been suggested by other authors (Ochoa Gonzalez and Weiss, 2015) who found that in the combustion process of coal-fired power plants, Zn isotopic signatures of the by-products depended on those of the feed materials. Thus, Zn isotopic signatures of slags were first impacted by the isotopic variability of the parental ores and secondly by the Rayleigh distillation during the smelting.

The copper isotopic signature of the collected coatings varied from −0.22 ± 0.04‰ (top) to −0.46 ± 0.01‰ (bottom). Slags showed a larger range of δ^{65}Cu values than those observed for Zn isotopes, varying from −1.70 ± 0.01‰ to 0.26 ± 0.02‰ ($n = 8$) (Fig. 3c, Tables S1c, d). δ^{65}Cu values of five out of eight slags were heavier (−0.11 ± 0.1‰ to 0.26 ± 0.02‰) than the chimney coating signature (−0.22 ± 0.04‰ (top)). However, three slags displayed a lighter isotopic enrichment (−1.08 ± 0.02‰; −1.70 ± 0.01‰; −1.34 ± 0.03‰) than the chimney coatings (Table S1d).

Previous studies showed that Cu is not affected by Rayleigh distillation (Bigalke et al., 2010; Gale et al., 1999) even in Cu smelters, since the Cu isotopic signatures of ash and slags are similar. The volatilization temperature of Cu is higher than that of Zn ($T°_{volatilization}$: 2595 °C and 907 °C, respectively). The smelting process temperature at the Escalette smelter varied between 1000 and 1150 °C (Carlier et al., 2010), thus allowing volatilization for Zn, but not for Cu. We thus hypothesize that the Cu isotopic heterogeneity found in slags mainly resulted from inputs of various galena-ores rather than from an isotopic distillation. No data are available for δ^{65}Cu values in galena ores to confirm this hypothesis, but Cu-S bearing ores (i.e. chalcopyrite and enargite) that are chemically close to the Pb-S (galena) ores processed by the smelter, display δ^{65}Cu values ranging from −1% to 1% (Mathur et al., 2009) that fit our measurements.

We measured different isotopic compositions at the bottom and the top of the chimney (Fig. 3b, Table S1c). Copper and Zn isotopic signatures of the bottom sample (δ^{65}Cu: −0.46 ± 0.01‰; δ^{66}Zn: −0.26 ± 0.09‰) were close to those measured for slags while the top sample was enriched in light Zn isotope (−0.70 ± 0.04‰), and heavy Cu isotope (−0.22 ± 0.04‰). We propose therefore that the Cu and Zn isotopic signatures of the chimney bottom sample are close to those of the processed ores like the slags; while in the top sample, isotopic signatures

were affected by Rayleigh distillation (for Zn) and equilibrium fractionation (for Cu) that occurred during transport in the vapor phase. A decrease in the plume temperature and condensation of particles during the vapor phase travelling as observed by (Ochoa Gonzalez and Weiss, 2015) in bottom and flying ash samples from a coal power plant could explain the differences in metal concentrations between the two extremities of the chimney. Like other smelters in the area at that time, the Escalette smelter is characterized by a long sub-horizontal conduit, built on the ground, and creeping up the hill along the ridge rather than by the short, vertical chimneys as found in modern smelters. Thus, interactions of Zn and Cu during transport in the vapor phase were maximized causing an enrichment in light Zn isotope and an enrichment in heavy Cu isotope (Balistrieri et al., 2008; Pokrovsky et al., 2008).

3.2. Assessing the extent of the soil contamination

3.2.1. Elemental concentrations: highlighting soil surface contamination

Trace metal concentrations in the soil profiles (Fig. 2 and Table S1c) were studied to determine the horizontal extent of metal contamination in the vicinity of the Escalette smelter. Surface horizons of the S1, S2, and S3 profiles were clearly affected by atmospheric deposition of metal-rich particles with Pb and Zn concentrations decreasing with increasing distance from the smelter and metal levels in the S1 A horizon up to 121× (Pb) and 14× (Zn) those found in the deep horizon of the more distant soil (S5 C) (Table S1c).

For all the studied soils, the surface horizons showed higher Pb, Zn, and Cu concentrations than deeper horizons except for S5 that had the lowest trace metal concentrations in the A horizons. All Zn and Pb concentrations were well above the values measured in five unpolluted local soils developed on calcareous parent materials (Austruy et al., 2016), both for the A topsoil (up to 22-fold for Zn and 39-fold for Pb) and for the subsoils (up to 3-fold for Zn and Pb). In S5, Zn concentrations were higher than those for natural calcareous soils in both surface (27 to 64 mg kg^{-1} (Austruy et al., 2016)) and deep horizons (19 to 59 mg kg^{-1} (Austruy et al., 2016)). However, Pb concentrations were lower than those estimated by (Austruy et al., 2016) both for surface (20 to 78 mg kg^{-1}) and deep horizons (9 to 42 mg kg^{-1}).

In all soils, Cu concentrations were low and close to geogenic values ranging from 4 mg kg^{-1} to 17 mg kg^{-1} (Austruy et al., 2016) compared to Zn and Pb (Fig. 2c). However, S1 displayed concentrations ~2.5× higher than S5 indicating a small potential contamination by smelter emissions. Soils displayed more homogenous Cu concentrations with a smaller depth-induced decrease that was most likely due to initially lower Cu concentrations in the parental limestone and to a low concentration in the source galena, thus in smelter emissions.

Although S2 was closer to the smelter than S3 (Fig. S1), Zn, Pb, and Cu concentrations were lower. This could be related to the fact that S2 was obscured from direct line of sight by a calcareous cliff that may have limited the deposition of metal-bearing airborne particles even with NNW winds that can reach up to 110 km h^{-1}.

High trace metal concentrations in surface horizons decreasing with depth are similar to patterns observed in uncontaminated soils (Legros, 2007). Furthermore, higher trace metal concentrations in deep horizons compared to other soils in the area could originate from a higher pedogeochemical background. Local variations in the natural pedogeochemical background can be determined from the relationship between total Fe and the trace metals and can provide information about a potential trace metal contamination (Baize and Sterckeman, 2001). In our soils, the relationship between total Fe and trace metals made it possible to distinguish between (i) a group of deep horizons having low trace metal concentrations and (ii) a group of surface horizons, with a high trace metal content for relatively low Fe concentrations. This approach revealed the horizontal extent of trace metal contamination of surface horizons in the Escalette area, but did not inform on the potential transfers of anthropogenic metals down the profiles and/or on the source contributions.

3.3. Isotopic signatures: tracing the smelter contamination in soil profiles

3.3.1. Lead

The surface horizons of all profiles showed Pb isotopic compositions similar to those of the chimney coatings and the slags, indicating that lead contamination originated from smelter emissions. In a $^{208}Pb/^{206}Pb$ vs $^{207}Pb/^{206}Pb$ plot (Fig. 4a), soils and chimney coatings lay along a linear trend corresponding to a mixing line between a radiogenic end-member (i.e. the emitted anthropogenic Pb), and an uncontaminated end-member characterized by a lower radiogenic Pb signature (i.e. the local pedogeochemical background) found in the S5 deepest horizon.

Lead isotopic ratios of the slags plotted out this $^{208}Pb/^{206}Pb$ vs $^{207}Pb/^{206}Pb$ mixing line (Fig. 4a) and demonstrate that slag-generated dust did not contribute to the soil contamination. Moreover, considering the local topography and the fact that these slags appeared as a solid unaltered material, it is unlikely that slag-related dust contaminated soils located at the top of the slopes. This observation supports the hypothesis that Pb contamination in soils was solely caused by the metal-rich particles emitted by the smelter. Furthermore, the chimney signature reflects the average composition of all the isotopic compositions of galena ores processed over time (Figs. 3a and 4a).

The limited variation of $^{208}Pb/^{206}Pb$ ratios with depth (Fig. 3a) or the soil profile distribution on the mixing line (Fig. 4a), indicates that (i) Pb contamination affected all soils from S1 to S5 (ii) Pb concentrations in soils resulted from two lead sources and (iii), anthropogenic Pb was transferred towards depth.

In Fig. 4a the S5 A horizon lies slightly off the mixing line, indicating that this sample received a contribution from another lead source other than the smelter, e.g. urban aerosols or modern industrial sources. Three-component mixing for this sample can also be identified in a

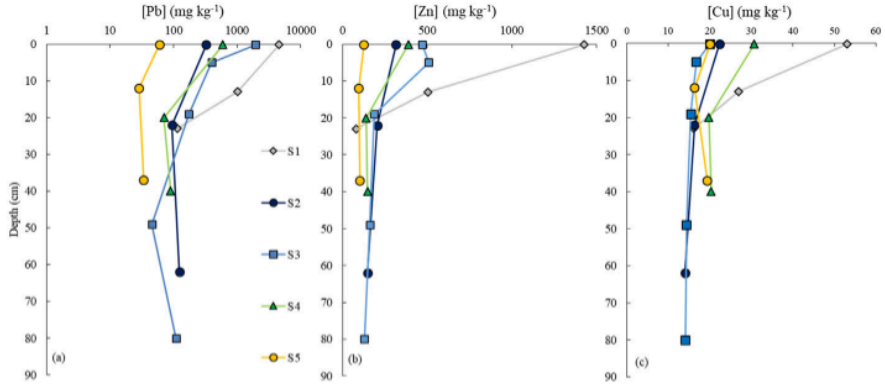

Fig. 2. Concentration (mg kg^{-1}) profiles of Pb (a), Zn (b) and Cu (c) in sampled soils. For Pb concentrations (a) note the logarithmic scale.

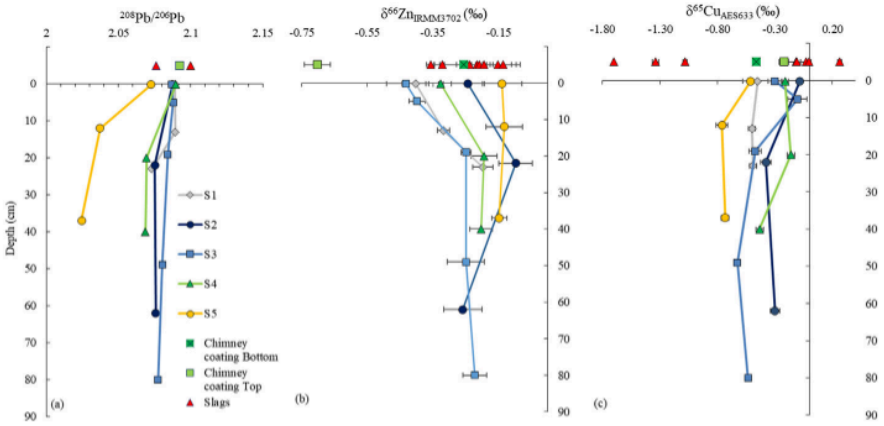

Fig. 3. Evolution of Pb (a), Zn (b) and Cu (c) isotopic signatures of soils with depth. For clarity, results obtained on the smelter samples (slags and chimney) are placed above the surface level. Error bars represent the two standard deviations (2SD) calculated from three analyses of the same sample. Calculated 2SD for Pb ratios are $<10^{-4}$ and are printed in smaller type than the symbols. In the $^{208}Pb/^{206}Pb$ plot (a), the two chimney coatings (top and bottom) overlap due to their identical Pb isotopic compositions. Soil sample symbols are placed at the top of their respective horizons. Only two slags (1,2) were analyzed for their Pb isotopic signatures while 7 slags were analyzed for Zn and Cu.

$^{208}Pb/^{204}Pb$ vs $^{206}Pb/^{204}Pb$ plot (Fig. 4b) as suggested by (Ellam, 2010). This source was not observed in other soils because of the dominant lead signature from the smelter particles. We hypothesize that this source may be representative of the atmospheric aerosols emitted by the combustion of fossil energy (i.e. road traffic in Marseilles) after the closing of the smelter.

Reconstruction of the lead isotopic signature of French (northern and southern) atmospheric aerosols since the 1980s, based on previously published data (Luck and Ben Othman, 2002; Maring et al., 1987; Véron et al., 1999), produced a mixing line ($r^2 = 0.95$; p value < 0.001) that did not intersect our S5 A horizon sample, but instead drove it away from the two end-member mixture (Fig. S4).

3.3.2. Zinc

Zinc isotopic signatures of the smelter samples (chimney) and the soil samples were different (Fig. 3b). The impact of light Zn-rich particles originating from the smelter could nonetheless be detected in the surface horizons.

Soil surface horizons from S1 to S4 showed $\delta^{66}Zn$ values ranging from -0.24 ± 0.05‰ to -0.43 ± 0.06‰ (Table S1c, Fig. 3b). The surface horizon of S5 had the heaviest Zn isotopic signature (-0.14 ± 0.06‰ Fig. 3b), that remained constant along the entire profile.

Isotope studies carried out on peat core sediments (Sonke et al., 2008) or on soils collected near a Zn or Cu smelter (Bigalke et al., 2010; Juillot et al., 2011), revealed a similar enrichment in light isotopes in the sediment/soil surface samples compared to those measured in the chimney stacks or smelter dust. However, these studies also noted discrepancies between Zn isotopic compositions of the smelter emissions and those of the sediment/soils. The discrepancy was explained by either mixing of the ash/dust signal with other emissions from different subunits of the smelter (Bigalke et al., 2010; Juillot et al., 2011) or by post-depositional fractionation (Juillot et al., 2011) that induced direct heavy enrichment in soils by Zn-sorption onto oxides and OM (Bryan et al., 2015; Guinoiseau et al., 2016; Jouvin et al., 2009; Juillot et al., 2008; Pokrovsky et al., 2005) or depletion in light isotopes by plant uptake (Aucour et al., 2015; Jouvin et al., 2012; Viers et al., 2007). This hypothesis was supported by other authors (Mattielli et al., 2009) who found a perfect match between Zn isotopic composition of the chimney dust and particles collected on dry plate rather than environmental (soil) samples, thus preventing any interactions with soil particles or plant uptake. Thus, the enrichment in heavy Zn isotopes in surface horizons of the studied soils could be explained by the direct (i.e. sorption) or the indirect (i.e. plant uptake) effect of post-deposition fractionation processes.

Soil profiles S1, S2, and S3 displayed isotopic variations with depth, up to $\Delta^{66}Zn_{S3\ A\ horizon\text{-}S3\ S\ horizon} = 0.21$‰ in S3 soil, and an increase in the $\delta^{66}Zn$ values down to ~0.2 m (Fig. 3b). $\delta^{66}Zn$ values of the deepest horizons of S1, S2, S3, and S4 were close to the isotopic signature of S5 and indicated that Zn contamination may have been limited at depth. Homogeneous Zn concentrations and $\delta^{66}Zn$ values in the S5 profile were (i) clearly distinct from those of the chimney and of the other soils, and (ii) fell within the range of previously published values for non-contaminated soils or continental rock parental material (−0.19 to 0.06‰) (Juillot et al., 2011; Pichat et al., 2003; Sonke et al., 2008; Wilkinson et al., 2005). Thus, we propose that the $\delta^{66}Zn$ value in S5 (~ −0.16‰) reflects the Zn isotopic signature of the local uncontaminated weathered parent material for the studied soil.

3.3.3. Copper

Given the proximity of S1, S2, and S3 to the chimney, a significant contribution of particle deposition on the Cu isotopic signatures in these soils was expected, especially for S1 where the Cu concentration was slightly higher in the A horizon (Fig. 2c). However, (i) Cu isotopic signatures in the A horizons of S1 and S5 are similar (Fig. 3c), and (ii) they did not reveal any similarities between soil surface and chimney coating unlike for Pb and Zn isotopes.

Except for S4, all profiles showed a similar vertical distribution, with an increasing light isotope contribution at depth as observed in (Bigalke et al., 2011; Mihaljevič et al., 2018) for natural soils. $\delta^{65}Cu$ values in deep horizons ranged from -0.30 ± 0.04‰ to -0.73 ± 0.03‰, values that are within the range of $\delta^{65}Cu$ values measured in unpolluted soils (−0.9 to 0.45‰ (Bigalke et al., 2011; Fekiacova et al., 2015; Kříbek et al., 2018).

We conclude that anthropogenic inputs of Cu from the smelter were negligible and observed Cu fractionation in the soil profiles was produced by pedogenetic processes. Two major processes are known to impact natural Cu isotopic signatures in soils: plant recycling (Jouvin et al., 2012; Weinstein et al., 2011) and interactions with solid mineral particles and/or solid organic matter (Balistrieri et al., 2008; Bigalke et al., 2011; Pokrovsky et al., 2008). These interactions cause direct (preferential sorption) and indirect (depletion of light isotopes by plant uptake) heavy isotope enrichment in soils. We propose that Cu concentrations in the soils were inherited from the parent material and higher Cu concentrations in the surface horizons resulted from Cu complexation to the organic matter. A ^{65}Cu enrichment observed in the surface horizons corroborates this hypothesis.

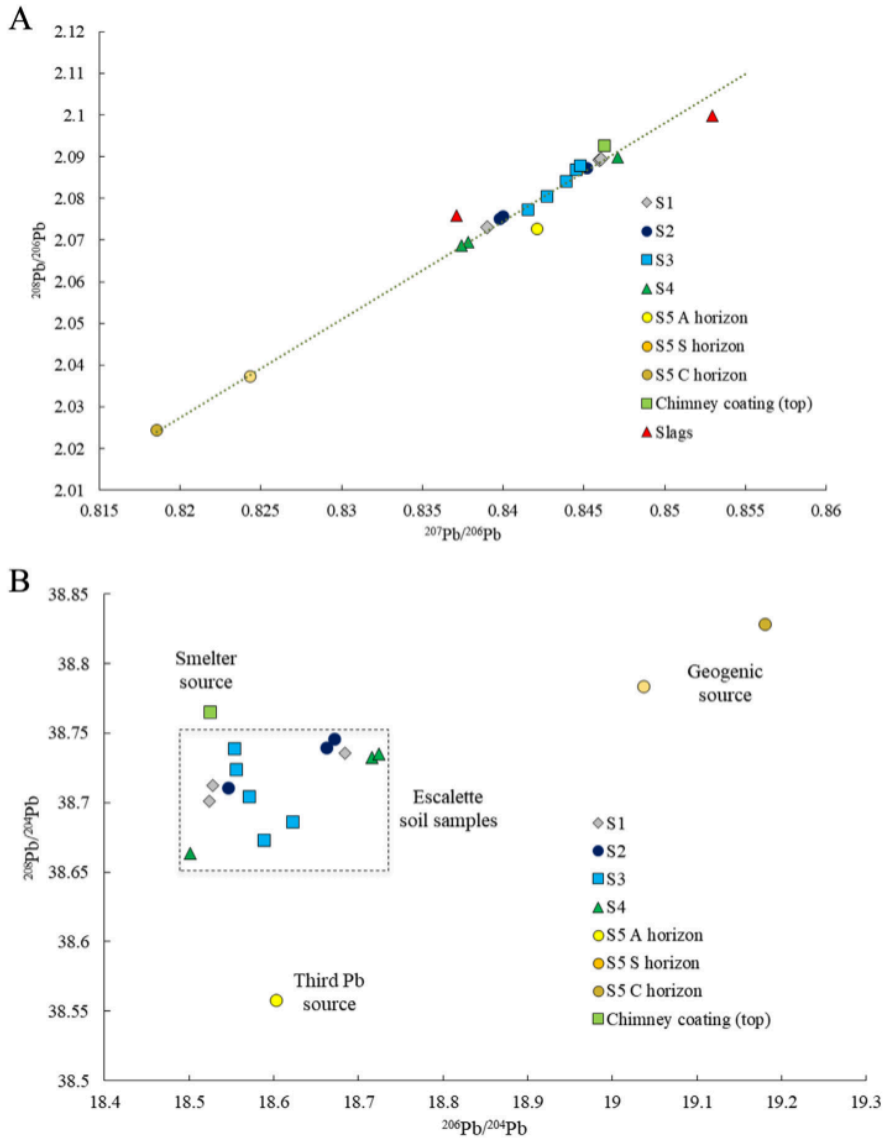

Fig. 4. a: Mixing trend of all sampled soils and smelter samples in a $^{208}Pb/^{206}Pb$ vs $^{207}Pb/^{206}Pb$ plot. Calculated 2SD for Pb ratios are $<10^{-4}$ and are printed in smaller type than the symbols. End members are represented by (i) the uncontaminated deepest horizon of the S5 profile (S5 C) and (ii) the chimney coatings. The dotted line represents the linear trend ($r^2 = 0.98$, p value < 0.001). For a given soil profile (except for S5), all horizons are represented by identical symbols. For S5, individual horizons are distinguished using the same symbols but different colors. Only slags 1 and 2 were analyzed for Pb isotopic compositions and are presented here (see Table S1c). b: Plot of $^{208}Pb/^{204}Pb$ vs $^{206}Pb/^{204}Pb$. Lead isotopes of the Escalette soil samples (highlighted by the dotted black square) are constrained in a three Pb source domain: smelter source (i.e. the chimney coating top), geogenic source (i.e. S5 deepest horizon) and a third source (i.e. atmospheric aerosol) only visible on the S5 A horizon. Calculated 2SD for Pb ratios are $<10^{-4}$ and printed smaller than the symbols. (For interpretation of the references to color in this figure legend, the reader is referred to the web version of this article.)

3.4. Long-term fate of anthropogenic Pb and Zn in soils

Emissions from the Escalette smelter and contamination started 167 years ago and lasted 74 years. Thus, the Escalette site provides a unique place to unravel the long-term fate of anthropogenic Pb and Zn in terms of remobilization/redistribution within the impacted soils.

3.4.1. Lead

The limited vertical variation of $^{208}Pb/^{206}Pb$ ratios (Fig. 3a) indicated that anthropogenic Pb, characterized by a high $^{208}Pb/^{206}Pb$ ratio (Table S1c), was transferred to depth from S1 to S4. Soluble transport of Pb in carbonated soil is limited because of the preferential precipitation of Pb as carbonates (cerussite, hydrocerussite or pyromorphite) at pH > 5.2 (Gee et al., 1997; Yanful et al., 1988). The pH of all studied soils ranged from 7.9 to 8.3 suggesting possible Pb carbonate precipitation, although no Pb carbonate was detected by XRD (probably due to concentrations below the detection limit). Considering the high distribution coefficient (*Kd*) of Pb for OM and Fe-oxides in poorly developed carbonated soils (Dumat et al., 2001; Lafuente et al., 2008), Pb is likely to occur as complexes with organic matter and soil minerals in the surface horizons of the studied soils. We hypothesized that Pb redistribution by colluvial processes could explain the results. However, erosion of upslope-contaminated-material and accumulation of eroded material downslope should be reflected by (i) Pb and Zn concentration peaks in subsurface horizons of downslope profiles, and (ii) abrupt changes in the Zn isotopic signatures of intermediate horizons towards light values caused by the integration of smelter-derived particles characterized by light $\delta^{66}Zn$ values. Since none of these effects were observed, we concluded that colluvial processes were not responsible for anthropogenic Pb migration.

Using a mixing model between two end-members (Figs. 4a and 5) represented by the deepest horizon of S5 (C) and the chimney coating (top) and based on the calculation proposed by (Phillips and Gregg, 2003), we can estimate the contribution of anthropogenic Pb to the total Pb pool in soils. We found that Pb-rich particles from the smelter (Fig. 5, Table S3) account for at least 91% of the total Pb pool measured in soil surface horizons from S1 to S4. The deepest soil horizons show the same trend with an anthropogenic Pb contribution estimated between 65 and 78% from S1 to S4.

The A horizon of S5 plotted out of the mixing line (Figs. 4a and 5) and the $^{208}Pb/^{204}Pb$ vs $^{206}Pb/^{204}Pb$ isotope plot confirmed the contribution of a third source of Pb in this sample (Fig. 4b). Thus, we used the Isosource program (Phillips and Gregg, 2003), provided by the Environmental Protection Agency, to calculate contributions of different Pb sources in a three end-member system (smelter, geogenic, atmospheric). The third Pb source considered in the system was urban aerosol, with values of $^{208}Pb/^{206}Pb = 2.1367$ and $^{207}Pb/^{206}Pb = 0.8944$, approximated by the Pb signature of Marseilles aerosols in 1987 (Maring et al., 1987).

According to these calculations, in S5 (the most distant soil from the smelter), the contribution of smelter-related anthropogenic Pb was best estimated at 39%, geogenic Pb at 42% and atmospheric Pb at 19%. The distributions of all possible contributions that satisfied the isotopic mass balance calculations are presented in (Fig. S5, Table S3).

This observation indicated that some Pb-rich particles from the smelter travelled up to 7 km SE. However, because of a lower concentration of the smelter-derived particles, Pb isotopic signature of S5 was significantly disturbed by inputs of atmospheric particles when smelter emissions stopped in 1925. At the other sites, the impact of atmospheric particles was not observable, most likely due to a higher content of smelter-derived particles.

The anthropogenic Pb contribution to total Pb decreased progressively with depth in all soils, excluding the impact of colluvial processes on Pb distribution in soils as stated above. Based on soil thickness, we calculated Pb penetration rates in soils ranging from 0.27 cm $year^{-1}$ (S1 soil) to 0.47 cm $year^{-1}$ (S3 soil) for a lower limit (i.e. calculated since the opening of the smelter, 167 years ago) or 0.48 cm $year^{-1}$ to 0.85 cm $year^{-1}$ in the same soils for the upper limit (i.e. calculated since the decommissioning of the smelter, 93 years ago). As Pb migration has been found to be facilitated by colloidal transport in contaminated soil (Amrhein et al., 1993; Denaix et al., 2001; Grolimund et al., 1996; Grolimund and Borkovec, 2005; Kretzschmar and Schafer, 2005) and because of both low Pb concentrations in the <0.2 μm soluble phase (Gelly et al. *in prep*) and low soil density, we propose that in the soils, this transfer occurred in the particulate form. Furthermore, metal migration could have been enhanced by bioturbation (Sterckeman et al., 2000), but we did not observe any evidence of significant worm activity to support this hypothesis.

3.4.2. Zinc

Zinc contamination was detected using Zn isotopes in all soils except S5. However, vertical variations in $\delta^{66}Zn$ values indicated that Zn mobility was different from that observed for Pb. Smelter-related Zn, characterized by light $\delta^{66}Zn$ values (Fig. 3b), accumulated within the A and A/C horizons. However, the observed shift towards heavier signatures in the studied soils demonstrates that another process modified the initial anthropogenic Zn signature. This shift could be attributed to (i) Zn adsorption or precipitation on organic matter and Al-Fe-Mn oxides (Balistrieri et al., 2008; Juillot et al., 2008; Pokrovsky et al., 2005) that would promote heavy isotope complexes, or to (ii) plant uptake that would deplete soil in light isotopes, thus enriching it in heavy ones (Aucour et al., 2015; Jouvin et al., 2012; Viers et al., 2007).

EXAFS results support the hypothesis of the transformation of anthropogenic Zn. In S1, Zn speciation could not be fitted by a simple combination of the chimney (anthropogenic contribution) and S5 compositions (natural contribution), indicating a change in the smelter-related Zn speciation after deposition onto the soil (Fig. S3b). EXAFS results highlighted the precipitation of a Zn-Layered Double Hydroxide (Zn-LDH) phase which was dominant (~77%, Table S2) in S1 topsoil, while in the S5 soil, Zn was mostly sorbed onto Fe and Mn oxides (Table S2). Zn-LDH precipitates have been identified as markers of Zn contamination in calcareous soils (Jacquat et al., 2008; Juillot et al., 2003; Voegelin et al., 2011) or other contaminated soils (Aucour et al., 2015; Voegelin et al., 2005). Zn-LDH precipitation occurs once all sorption sites have been saturated (Luxton et al., 2013) and is kinetically favored over precipitation of Zn-phyllosilicates, although these precipitates are also thermodynamically stable (Voegelin et al., 2005). The availability of Al and Si (Jacquat et al., 2008; Voegelin et al., 2005) and increasing Zn concentrations in soils seem to play a major role in the formation of Zn-LDH. No occurrences of Zn-LDH in Pb and/or Zn smelter exhausts have been reported in the literature. Similarly, we did not detect these compounds in the Escalette chimney (Table S2), most likely indicating unfavorable physico-chemical conditions in the chimney (e.g. more acidic pH).

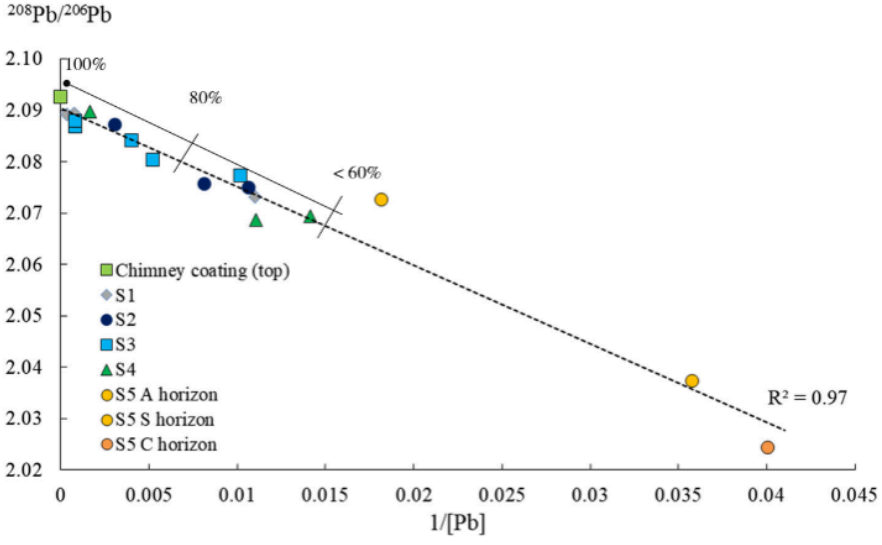

Fig. 5. Plot of $^{208}Pb/^{206}Pb$ vs 1/[Pb] total concentrations. A two end-member mixing line (dotted line, $r^2 = 0.97$; p value < 0.001) connects the chimney sample (top) and the deepest horizon of the S5 profile (C). Soils from S1 to S4 plotted along the mixing line, indicating that their total Pb concentrations represent a mixture of anthropogenic Pb from the smelter ($^{208}Pb/^{206}Pb$: 2.0922), and natural Pb, from the geogenic background ($^{208}Pb/^{206}Pb$: 2.0243). The contribution of anthropogenic Pb to the total Pb (%), presented in Table S3, is reported as a solid black line, close to the mixing line.

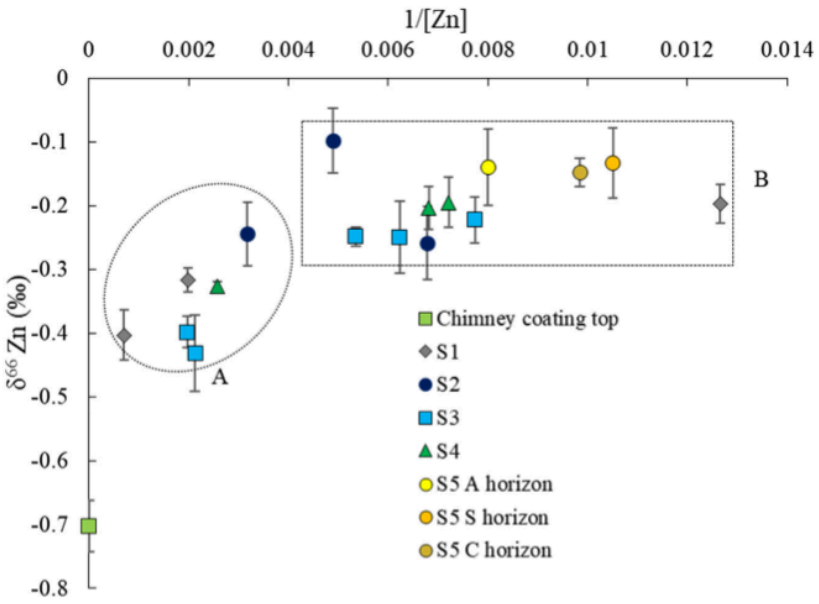

Fig. 6. Plot of δ^{66}Zn values (‰) vs 1/[Zn]. Zinc isotopic signatures of the soils cannot be explained by binary mixing. Two distinct Zn pools, labeled A and B, and highlighted by a circle and rectangle in dashed lines can be distinguished. Error bars represent the 2SD associated to δ^{66}Zn values. A: pool dominated by anthropogenic Zn from the smelter, observed in S1, S2, S3 and S4 surface horizons. Discrepancy between δ^{66}Zn values of the soils and the chimney sample can be explained by isotopic fractionation during precipitation of Zn-Layered-Double-Hydroxide in the surface horizons. B: pool dominated by natural Zn observed in all other subsurface horizons and in the S5 soil profile and originating from the natural geogenic background modified by pedogenetic processes.

Thus, Zn-LDH formation was considered to have contributed to (i) precipitation of smelter-related Zn in the S1 surface horizon, and (ii) alteration of the Zn isotopic signatures of the emitted particles by favoring heavy isotope complexes. Owing to the similarity in the Zn isotopic signature of the A horizons in S1 to S4, the same process may have occurred in all studied soils.

The mixing model calculated for Zn (like the model calculated for Pb) did not show any progressive mixing between the two end-members, but rather highlighted two Zn pools. One pool was represented by the surface horizons of soils from S1 to S4, the second one was represented by the deepest horizons of these soils and by the entire S5 profile (Fig. 6). Separation of the Zn pools confirmed that anthropogenic Zn accumulated in surface horizons and that precipitation of the Zn-LDH prevented leaching of Zn towards deeper horizons. Consequently, at depth, Zn is considered to be of geogenic origin (inherited from the parental limestone).

Zinc isotopes confirmed that few Zn-rich particles reached S5 as their impact was not recorded by the δ^{66}Zn values, probably because anthropogenic Zn was incorporated in soils through pedogenetic processes as illustrated by EXAFS analyses (Table S2).

4. Conclusion

We used isotopic analyses to shed light on the behavior and transfer in soils of Pb, Zn, and Cu emitted simultaneously from the Escalette smelter, for 93 years. In contrast to Pb and Zn, Cu isotopes showed no evidence of Cu contamination of the soils in the vicinity of the Escalette smelter.

We recovered traces of smelter emissions in the soil surface (Zn-Pb) up to 7 km away from the smelter and at depth (Pb). The vertical mobility of anthropogenic Pb contrasts with previously published data on calcareous soils where Pb was immobilized in surface horizons.

In contrast, immobilization of smelter-related Zn within the surface horizons was documented by the shift in δ^{66}Zn values in soils compared to those of the chimney coatings, representing the proxy used for the isotopic signatures of the emitted particles. This is explained by the precipitation of Zn-LDH, typical of Zn-rich environments with near-neutral to slightly basic pH. This form of Zn was different from those observed in the chimney coatings and in S5, indicating that (i) speciation of Zn emitted from the smelter changed after deposition, altering Zn isotopic signatures, and (ii) fewer Zn-rich particles reached S5 and were included in the biogeochemical cycle of Zn through pedogenetic processes.

However, the role of vegetation in the anthropogenic Zn cycling at this site needs to be deciphered in future studies. Particularly, *in natura* isotopic measurements could shed light on how the vegetation adapts to anthropogenic metals and incorporates them into its biogeochemical cycle. This work underlines the complementarity of elemental, isotopic, and speciation analyses for tracing and unravelling the fate of historical multi-metal contamination in soils by providing a complementary set of data that highlights the distinctive behavior of trace metals originating from a common industrial source.

Acknowledgement

The authors wish to thank A. Véron for useful insights on Pb isotopes, D. Borschneck for support on XRD measurements, B. Angeletti for Q-ICP-MS analyses, and P. Höhener for critically reading the manuscript. We thank the anonymous reviewers for their constructive reviews that helped improve the manuscript. This work was supported by the following projects: Agence Nationale de la Recherche (ANR, France) project EQUIPEX ASTER-CEREGE, Pari Scientifique EA-INRA (COMETICS), ANR project MARSECO (CES018-2008), Labex DRIIHM, French Program "Investissements d'avenir" (ANR-11-LABX-0010). We acknowledge the European Synchrotron Radiation Facility (ESRF) for the provision of synchrotron beam time.

Appendix A. Supplementary data

Supplementary data to this article can be found online at https://doi.org/10.1016/j.scitotenv.2019.02.092.

References

Addinsoft, 2016. XLSTAT 2016: Data Analysis and Statistical Solution for Microsoft Excel.
Affholder, M.-C., Prudent, P., Masotti, V., Coulomb, B., Rabier, J., Nguyen-The, B., Laffont-Schwob, I., 2013. Transfer of metals and metalloids from soil to shoots in wild rosemary (Rosmarinus officinalis L.) growing on a former lead smelter site: human

exposure risk. Sci. Total Environ. 454–455, 219–229. https://doi.org/10.1016/j.scitotenv.2013.02.086.
Amrhein, C., Mosher, P.A., Strong, J.E., 1993. Colloid-assisted transport of trace metals in roadside soils receiving deicing salts. Soil Sci. Soc. Am. J. 57, 1212. https://doi.org/10.2136/sssaj1993.03615995005700050009x.
Araújo, D.F., Machado, W., Weiss, D., Mulholland, D.S., Garnier, J., Souto-Oliveira, C.E., Babinski, M., 2018. Zinc isotopes as tracers of anthropogenic sources and biogeochemical processes in contaminated mangroves. Appl. Geochem. 95, 25–32. https://doi.org/10.1016/j.apgeochem.2018.05.008.
Aucour, A.-M., Bedell, J.-P., Queyron, M., Magnin, V., Testemale, D., Sarret, G., 2015. Dynamics of Zn in an urban wetland soil–plant system: coupling isotopic and EXAFS approaches. Geochim. Cosmochim. Acta 160, 55–69. https://doi.org/10.1016/j.gca.2015.03.040.
Austruy, A., Dron, J., Charbonnier, E., Babaguela, N., Miche, H., Keller, C., Chamaret, P., 2016. Teneurs naturelles et apports anthropiques en éléments traces dans les sols à l'ouest de l'étang de Berre. Etude Gest. Sols 18.
Baize, D., Sterckeman, T., 2001. Of the necessity of knowledge of the natural pedo-geochemical background content in the evaluation of the contamination of soils by trace elements. Sci. Total Environ. 264, 127–139. https://doi.org/10.1016/S0048-9697(00)00615-X.
Baize, D., Girard, M.-C., et al., 2009. Référentiel pédologique 2008. Quae.
Balistrieri, L.S., Borrok, D.M., Wanty, R.B., Ridley, W.I., 2008. Fractionation of Cu and Zn isotopes during adsorption onto amorphous Fe(III) oxyhydroxide: Experimental mixing of acid rock drainage and ambient river water. Geochim. Cosmochim. Acta 72, 311–328. https://doi.org/10.1016/j.gca.2007.11.013.
Bigalke, M., Weyer, S., Kobza, J., Wilcke, W., 2010. Stable Cu and Zn isotope ratios as tracers of sources and transport of Cu and Zn in contaminated soil. Geochim. Cosmochim. Acta 74, 6801–6813. https://doi.org/10.1016/j.gca.2010.08.044.
Bigalke, M., Weyer, S., Wilcke, W., 2011. Stable Cu isotope fractionation in soils during oxic weathering and podzolization. Geochim. Cosmochim. Acta 75, 3119–3134. https://doi.org/10.1016/j.gca.2011.03.005.
Borrok, D.M., Wanty, R.B., Ian Ridley, W., Lamothe, P.J., Kimball, B.A., Verplanck, P.L., Runkel, R.L., 2009. Application of iron and zinc isotopes to track the sources and mechanisms of metal loading in a mountain watershed. Appl. Geochem. 24, 1270–1277. https://doi.org/10.1016/j.apgeochem.2009.03.010.
Bryan, A.L., Dong, S., Wilkes, E.B., Wasylenki, L.E., 2015. Zinc isotope fractionation during adsorption onto Mn oxyhydroxide at low and high ionic strength. Geochim. Cosmochim. Acta 157, 182–197. https://doi.org/10.1016/j.gca.2015.01.026.
Carlier, C.M.-L., Ploquin, A., Fluck, P., 2010. Apport de la géochimie et de la pétrologie à la connaissance de la métallurgie primaire du plomb argentifère au Moyen Âge: Les exemples du Mont Lozère (Cévennes) et de Pfaffenloch (Vosges). ArchéoSciences, 159–176 https://doi.org/10.4000/archeosciences.2728.
Chapman, J.B., Mason, T.F.D., Weiss, D.J., Coles, B.J., Wilkinson, J.J., 2006. Chemical separation and isotopic variations of Cu and Zn from five geological reference materials. Geostand. Geoanal. Res. 30, 5–16. https://doi.org/10.1111/j.1751-908X.2006.tb00907.x.
Cloquet, C., Carignan, J., Libourel, G., Sterckeman, T., Perdrix, E., 2006. Tracing source pollution in soils using cadmium and lead isotopes. Environ. Sci. Technol. 40, 2525–2530. https://doi.org/10.1021/es052232+.
Cui, J., Wu, X., 2011. An experimental investigation on lead isotopic fractionation during metallurgical processes. Archaeometry 53, 205–214. https://doi.org/10.1111/j.1475-4754.2010.00548.x.
Daumalin, X., Raveux, O., 2016. A region scarred by pollution. In: Xavier Daumalin, I.L.-S. (Ed.), Es Calanques Industrielles de Marseille et Leurs Pollutions. Une Histoire Au Présent. REF.2C éditions, pp. 131–203.
Denaix, L., Semlali, R.M., Douay, F., 2001. Dissolved and colloidal transport of Cd, Pb, and Zn in a silt loam soil affected by atmospheric industrial deposition. Environ. Pollut. 10.
Desenfant, F., Veron, A.J., Camoin, G.F., Nyberg, J., 2006. Reconstruction of pollutant lead invasion into the tropical North Atlantic during the twentieth century. Coral Reefs 25, 473–484. https://doi.org/10.1007/s00338-006-0113-x.
Doelsch, E., Masion, A., Borschneck, D., Hazemann, J.-L., Saint Macary, H., Bottero, J.-Y., Rose, J., Basile-Doelsch, I., 2006. New combination of EXAFS spectroscopy and density fractionation for the speciation of chromium within an andosol. Environ. Sci. Technol. 40, 7602–7608. https://doi.org/10.1021/es060906q.
Dumat, C., Chiquet, A., Gooddy, D., Aubry, E., Morin, G., Juillot, F., Benedetti, M.F., 2001. Metal ion geochemistry in smelter impacted soils and soil solutions. Bull. Soc. Geol. Fr. 172, 539–548. https://doi.org/10.2113/172.5.539.
Ellam, R.M., 2010. The graphical presentation of lead isotope data for environmental source apportionment. Sci. Total Environ. 408, 3490–3492. https://doi.org/10.1016/j.scitotenv.2010.03.037.
Erel, Y., Veron, A., Halicz, L., 1997. Tracing the transport of anthropogenic lead in the atmosphere and in soils using isotopic ratios. Geochim. Cosmochim. Acta 61, 4495–4505. https://doi.org/10.1016/S0016-7037(97)00353-0.
World reference base for soil resources 2006: a framework for international classification, correlation and communication. In: FAO (Ed.), World Soil Resources Reports. FAO, Rome.
Fekiacova, Z., Abouchami, W., Galer, S.J.G., Garcia, M.O., Hofmann, A.W., 2007. Origin and temporal evolution of Ko'olau Volcano, Hawai'i: inferences from isotope data on the Ko'olau Scientific Drilling Project (KSDP), the Honolulu Volcanics and ODP Site 843. Earth Planet. Sci. Lett. 261, 65–83. https://doi.org/10.1016/j.epsl.2007.06.005.
Fekiacova, Z., Cornu, S., Pichat, S., 2015. Tracing contamination sources in soils with Cu and Zn isotopic ratios. Sci. Total Environ. 517, 96–105. https://doi.org/10.1016/j.scitotenv.2015.02.046.
Formentini, T.A., Legros, S., Fernandes, C.V.S., Pinheiro, A., Le Bars, M., Levard, C., Mallmann, F.J.K., da Veiga, M., Doelsch, E., 2017. Radical change of Zn speciation in pig slurry amended soil: key role of nano-sized sulfide particles. Environ. Pollut. 222, 495–503. https://doi.org/10.1016/j.envpol.2016.11.056.
Gale, N., Woodhead, A., Stos-Gale, Z., Walder, A., Bowen, I., 1999. Natural variations detected in the isotopic composition of copper: possible applications to archaeology and geochemistry. Int. J. Mass Spectrom. 184, 1–9. https://doi.org/10.1016/S1387-3806(98)14294-X.
Gee, C., Ramsey, M.H., Maskall, J., Thornton, I., 1997. Mineralogy and weathering processes in historical smelting slags and their effect on the mobilisation of lead. J. Geochem. Explor. 58, 249–257. https://doi.org/10.1016/S0375-6742(96)00062-3.
George, L., Cook, N.J., Ciobanu, C.L., Wade, B.P., 2015. Trace and minor elements in galena: a reconnaissance LA-ICP-MS study. Am. Mineral. 100, 548–569. https://doi.org/10.2138/am-2015-4862.
Grolimund, D., Borkovec, M., 2005. Colloid-facilitated transport of strongly sorbing contaminants in natural porous media: mathematical modeling and laboratory column experiments. Environ. Sci. Technol. 39, 6378–6386. https://doi.org/10.1021/es050207y.
Grolimund, D., Borkovec, M., Barmettler, K., Sticher, H., 1996. Colloid-facilitated transport of strongly sorbing contaminants in natural porous media: a laboratory column study. Environ. Sci. Technol. 30, 3118–3123. https://doi.org/10.1021/es960246x.
Guinoiseau, D., Gélabert, A., Moureau, J., Louvat, P., Benedetti, M.F., 2016. Zn isotope fractionation during sorption onto kaolinite. Environ. Sci. Technol. 50, 1844–1852. https://doi.org/10.1021/acs.est.5b05347.
Hamelin, B., Ferrand, J.L., Alleman, L., Nicolas, E., Veron, A., 1997. Isotopic evidence of pollutant lead transport from North America to the subtropical North Atlantic gyre. Geochim. Cosmochim. Acta 61, 4423–4428. https://doi.org/10.1016/S0016-7037(97)00242-1.
Jacquat, O., Voegelin, A., Villard, A., Marcus, M.A., Kretzschmar, R., 2008. Formation of Zn-rich phyllosilicate, Zn-layered double hydroxide and hydrozincite in contaminated calcareous soils. Geochim. Cosmochim. Acta 72, 5037–5054. https://doi.org/10.1016/j.gca.2008.07.024.
Jeon, S., Kwon, M.J., Yang, J., Lee, S., 2017. Identifying the source of Zn in soils around a Zn smelter using Pb isotope ratios and mineralogical analysis. Sci. Total Environ. 601–602, 66–72. https://doi.org/10.1016/j.scitotenv.2017.05.181.
Jouvin, D., Louvat, P., Juillot, F., Maréchal, C.N., Benedetti, M.F., 2009. Zinc isotopic fractionation: why organic matters. Environ. Sci. Technol. 43, 5747–5754. https://doi.org/10.1021/es803012e.
Jouvin, D., Weiss, D.J., Mason, T.F.M., Bravin, M.N., Louvat, P., Zhao, F., Ferec, F., Hinsinger, P., Benedetti, M.F., 2012. Stable isotopes of Cu and Zn in higher plants: evidence for Cu reduction at the root surface and two conceptual models for isotopic fractionation processes. Environ. Sci. Technol. 46, 2652–2660. https://doi.org/10.1021/es202587m.
Juillot, F., Morin, G., Ildefonse, P., Trainor, T.P., Benedetti, M., Galoisy, L., Calas, G., Brown, G.E., 2003. Occurrence of Zn/Al hydrotalcite in smelter-impacted soils from northern France: evidence from EXAFS spectroscopy and chemical extractions. Am. Mineral. 88, 509–526. https://doi.org/10.2138/am-2003-0405.
Juillot, F., Maréchal, C., Ponthieu, M., Cacaly, S., Morin, G., Benedetti, M., Hazemann, J.L., Proux, O., Guyot, F., 2008. Zn isotopic fractionation caused by sorption on goethite and 2-Lines ferrihydrite. Geochim. Cosmochim. Acta 72, 4886–4900. https://doi.org/10.1016/j.gca.2008.07.007.
Juillot, F., Maréchal, C., Morin, G., Jouvin, D., Cacaly, S., Telouk, P., Benedetti, M.F., Ildefonse, P., Sutton, S., Guyot, F., Brown, G.E., 2011. Contrasting isotopic signatures between anthropogenic and geogenic Zn and evidence for post-depositional fractionation processes in smelter-impacted soils from Northern France. Geochim. Cosmochim. Acta 75, 2295–2308. https://doi.org/10.1016/j.gca.2011.02.004.
Kabata-Pendias, A., 2011. Trace Elements in Soils and Plants. Fourth edition. p. 33.
Kimball, B.E., Mathur, R., Dohnalkova, A.C., Wall, A.J., Runkel, R.L., Brantley, S.L., 2009. Copper isotope fractionation in acid mine drainage. Geochim. Cosmochim. Acta 73, 1247–1263. https://doi.org/10.1016/j.gca.2008.11.035.
Kretzschmar, R., Schafer, T., 2005. Metal retention and transport on colloidal particles in the environment. Elements 1, 205–210. https://doi.org/10.2113/gselements.1.4.205.
Kříbek, B., Šípková, A., Ettler, V., Mihaljevič, M., Majer, V., Knésl, I., Mapani, B., Penížek, V., Vaněk, A., Sracek, O., 2018. Variability of the copper isotopic composition in soil and grass affected by mining and smelting in Tsumeb, Namibia. Chem. Geol. https://doi.org/10.1016/j.chemgeo.2018.05.035.
Lafuente, A.L., González, C., Quintana, J.R., Vázquez, A., Romero, A., 2008. Mobility of heavy metals in poorly developed carbonate soils in the Mediterranean region. Geoderma 145, 238–244. https://doi.org/10.1016/j.geoderma.2008.03.012.
Legros, J.P., 2007. Les grands sols du monde, Science & technologie de l'environnement. Presses polytechniques et universitaires romandes.
Legros, S., Levard, C., Marcato-Romain, C.-E., Guiresse, M., Doelsch, E., 2017. Anaerobic digestion alters copper and zinc speciation. Environ. Sci. Technol. 51, 10326–10334. https://doi.org/10.1021/acs.est.7b01662.
Luck, J.M., Ben Othman, D., 2002. Trace element and Pb isotope variability during rainy events in the NW Mediterranean: constraints on anthropogenic and natural sources. Chem. Geol. 182, 443–460. https://doi.org/10.1016/S0009-2541(01)00324-2.
Lugmair, G., Galer, S.J., 1992. Age and isotopic relationships among the angrites Lewis Cliff 86010 and Angra dos Reis. Geochim. Cosmochim. Acta 56, 1673–1694. https://doi.org/10.1016/0016-7037(92)90234-A.
Luxton, T.P., Miller, B.W., Scheckel, K.G., 2013. Zinc Speciation Studies in Soil, Sediment and Environmental Samples. p. 45.
Maréchal, C.N., Télouk, P., Albarède, F., 1999. Precise analysis of copper and zinc isotopic compositions by plasma-source mass spectrometry. Chem. Geol. 156, 251–273. https://doi.org/10.1016/S0009-2541(98)00191-0.
Maring, H., Settle, D.M., Buat-Ménard, P., Dulac, F., Patterson, C.C., 1987. Stable lead isotope tracers of air mass trajectories in the Mediterranean region. Nature 330, 154.
Mathur, R., Titley, S., Barra, F., Brantley, S., Wilson, M., Phillips, A., Munizaga, F., Maksaev, V., Vervoort, J., Hart, G., 2009. Exploration potential of Cu isotope fractionation in porphyry copper deposits. J. Geochem. Explor. 102, 1–6. https://doi.org/10.1016/j.gexplo.2008.09.004.

Mattielli, N., Petit, J.C.J., Deboudt, K., Flament, P., Perdrix, E., Taillez, A., Rimetz-Planchon, J., Weis, D., 2009. Zn isotope study of atmospheric emissions and dry depositions within a 5 km radius of a Pb–Zn refinery. Atmos. Environ. 43, 1265–1272. https://doi.org/10.1016/j.atmosenv.2008.11.030.

Mihaljevič, M., Jarošíková, A., Ettler, V., Vaněk, A., Penížek, V., Kříbek, B., Chrastný, V., Sracek, O., Trubač, J., Svoboda, M., Nyambe, I., 2018. Copper isotopic record in soils and tree rings near a copper smelter, Copperbelt, Zambia. Sci. Total Environ. 621, 9–17. https://doi.org/10.1016/j.scitotenv.2017.11.114.

Ochoa Gonzalez, R., Weiss, D., 2015. Zinc isotope variability in three coal-fired power plants: a predictive model for determining isotopic fractionation during combustion. Environ. Sci. Technol. 49, 12560–12567. https://doi.org/10.1021/acs.est.5b02402.

Opfergelt, S., Cornélis, J.T., Houben, D., Givron, C., Burton, K.W., Mattielli, N., 2017. The influence of weathering and soil organic matter on Zn isotopes in soils. Chem. Geol. 466, 140–148. https://doi.org/10.1016/j.chemgeo.2017.06.002.

Phillips, D.L., Gregg, J.W., 2003. Source partitioning using stable isotopes: coping with too many sources. Oecologia 136, 261–269. https://doi.org/10.1007/s00442-003-1218-3.

Pichat, S., Douchet, C., Albarède, F., 2003. Zinc isotope variations in deep-sea carbonates from the eastern equatorial Pacific over the last 175 ka. Earth Planet. Sci. Lett. 210, 167–178. https://doi.org/10.1016/S0012-821X(03)00106-7.

Pokrovsky, O.S., Viers, J., Freydier, R., 2005. Zinc stable isotope fractionation during its adsorption on oxides and hydroxides. J. Colloid Interface Sci. 291, 192–200. https://doi.org/10.1016/j.jcis.2005.04.079.

Pokrovsky, O.S., Viers, J., Emnova, E.E., Kompantseva, E.I., Freydier, R., 2008. Copper isotope fractionation during its interaction with soil and aquatic microorganisms and metal oxy(hydr)oxides: possible structural control. Geochim. Cosmochim. Acta 72, 1742–1757. https://doi.org/10.1016/j.gca.2008.01.018.

Ravel, B., Newville, M., 2005. ıt ATHENA, ıt ARTEMIS, ıt HEPHAESTUS: data analysis for X-ray absorption spectroscopy using ıt IFEFFIT. J. Synchrotron Radiat. 12, 537–541. https://doi.org/10.1107/S0909049505012719.

Semlali, R.M., van Oort, F., Denaix, L., Loubet, M., 2001. Estimating distributions of endogenous and exogenous Pb in soils by using Pb isotopic ratios. Environ. Sci. Technol. 35, 4180–4188. https://doi.org/10.1021/es0002621.

Shiel, A.E., Weis, D., Orians, K.J., 2010. Evaluation of zinc, cadmium and lead isotope fractionation during smelting and refining. Sci. Total Environ. 408, 2357–2368. https://doi.org/10.1016/j.scitotenv.2010.02.016.

Shotyk, W., Weiss, D., Heisterkamp, M., Cheburkin, A.K., Appleby, P.G., Adams, F.C., 2002. New peat bog record of atmospheric lead pollution in Switzerland: Pb concentrations, enrichment factors, isotopic composition, and organolead species. Environ. Sci. Technol. 36, 3893–3900. https://doi.org/10.1021/es010196i.

Šillerová, H., Chrastný, V., Vítková, M., Francová, A., Jehlička, J., Gutsch, M.R., Kocourková, J., Aspholm, P.E., Nilsson, L.O., Berglen, T.F., Jensen, H.K.B., Komárek, M., 2017. Stable isotope tracing of Ni and Cu pollution in North-East Norway: potentials and drawbacks. Environ. Pollut. 228, 149–157. https://doi.org/10.1016/j.envpol.2017.05.030.

Sivry, Y., Riotte, J., Sonke, J.E., Audry, S., Schäfer, J., Viers, J., Blanc, G., Freydier, R., Dupré, B., 2008. Zn isotopes as tracers of anthropogenic pollution from Zn-ore smelters The Riou Mort–Lot River system. Chem. Geol. 255, 295–304. https://doi.org/10.1016/j.chemgeo.2008.06.038.

Song, S., Mathur, R., Ruiz, J., Chen, D., Allin, N., Guo, K., Kang, W., 2016. Fingerprinting two metal contaminants in streams with Cu isotopes near the Dexing Mine, China. Sci. Total Environ. 544, 677–685. https://doi.org/10.1016/j.scitotenv.2015.11.101.

Sonke, J., Sivry, Y., Viers, J., Freydier, R., Dejonghe, L., Andre, L., Aggarwal, J., Fontan, F., Dupre, B., 2008. Historical variations in the isotopic composition of atmospheric zinc deposition from a zinc smelter. Chem. Geol. 252, 145–157. https://doi.org/10.1016/j.chemgeo.2008.02.006.

Sossi, P.A., Halverson, G.P., Nebel, O., Eggins, S.M., 2015. Combined separation of Cu, Fe and Zn from rock matrices and improved analytical protocols for stable isotope determination. Geostand. Geoanal. Res. 39, 129–149. https://doi.org/10.1111/j.1751-908X.2014.00298.x.

Souto-Oliveira, C.E., Babinski, M., Araújo, D.F., Andrade, M.F., 2018. Multi-isotopic fingerprints (Pb, Zn, Cu) applied for urban aerosol source apportionment and discrimination. Sci. Total Environ. 626, 1350–1366. https://doi.org/10.1016/j.scitotenv.2018.01.192.

Sterckeman, T., Douay, F., Proix, N., Fourrier, H., 2000. Vertical distribution of Cd, Pb and Zn in soils near smelters in the North of France. Environ. Pollut. 107, 377–389. https://doi.org/10.1016/S0269-7491(99)00165-7.

Stos-Gale, Z., Gale, N.H., Houghton, J., Speakman, R., 1995. Lead isotope data from the Isotrace Laboratory, Oxford: archaeometry data base 1, ores from the western Mediterranean. Archaeometry 37, 407–415. https://doi.org/10.1111/j.1475-4754.1995.tb00753.x.

Testiati, E., Parinet, J., Massiani, C., Laffont-Schwob, I., Rabier, J., Pfeifer, H.-R., Lenoble, V., Masotti, V., Prudent, P., 2013. Trace metal and metalloid contamination levels in soils and in two native plant species of a former industrial site: evaluation of the phytostabilization potential. J. Hazard. Mater. 248–249, 131–141. https://doi.org/10.1016/j.jhazmat.2012.12.039.

Thapalia, A., Borrok, D.M., Van Metre, P.C., Musgrove, M., Landa, E.R., 2010. Zn and Cu isotopes as tracers of anthropogenic contamination in a sediment core from an urban lake. Environ. Sci. Technol. 44, 1544–1550. https://doi.org/10.1021/es902933y.

Véron, A., Flament, P., Bertho, M.L., Alleman, L., Flegal, R., Hamelin, B., 1999. Isotopic evidence of pollutant lead sources in northwestern France. Atmos. Environ. 33, 3377–3388. https://doi.org/10.1016/S1352-2310(98)00376-8.

Viers, J., Oliva, P., Nonell, A., Gélabert, A., Sonke, J.E., Freydier, R., Gainville, R., Dupré, B., 2007. Evidence of Zn isotopic fractionation in a soil–plant system of a pristine tropical watershed (Nsimi, Cameroon). Chem. Geol. 239, 124–137. https://doi.org/10.1016/j.chemgeo.2007.01.005.

Viers, J., Grande, J.A., Zouiten, C., Freydier, R., Masbou, J., Valente, T., de la Torre, M.-L., Destrigneville, C., Pokrovsky, O.S., 2018. Are Cu isotopes a useful tool to trace metal sources and processes in acid mine drainage (AMD) context? Chemosphere 193, 1071–1079. https://doi.org/10.1016/j.chemosphere.2017.11.133.

Voegelin, A., Pfister, S., Scheinost, A.C., Marcus, M.A., Kretzschmar, R., 2005. Changes in zinc speciation in field soil after contamination with zinc oxide. Environ. Sci. Technol. 39, 6616.

Voegelin, A., Jacquat, O., Pfister, S., Barmettler, K., Scheinost, A.C., Kretzschmar, R., 2011. Time-dependent changes of zinc speciation in four soils contaminated with zincite or sphalerite. Environ. Sci. Technol. 45, 255–261. https://doi.org/10.1021/es101189d.

von Storch, H., Costa-Cabral, M., Hagner, C., Feser, F., Pacyna, J., Pacyna, E., Kolb, S., 2003. Four decades of gasoline lead emissions and control policies in Europe: a retrospective assessment. Sci. Total Environ. 311, 151–176. https://doi.org/10.1016/S0048-9697(03)00051-2.

Weinstein, C., Moynier, F., Wang, K., Paniello, R., Foriel, J., Catalano, J., Pichat, S., 2011. Isotopic fractionation of Cu in plants. Chem. Geol. https://doi.org/10.1016/j.chemgeo.2011.05.010.

Weiss, D., Shotyk, W., Boyle, E.A., Kramers, J.D., Appleby, P.G., Cheburkin, A.K., 2002. Comparative study of the temporal evolution of atmospheric lead deposition in Scotland and eastern Canada using blanket peat bogs. Sci. Total Environ. 292, 7–18. https://doi.org/10.1016/S0048-9697(02)00025-6.

Weiss, D.J., Rehkdmper, M., Schoenberg, R., McLaughlin, M., Kirby, J., Campbell, P.G.C., Arnold, T., Chapman, J., Peel, K., Gioia, A.S., 2008. Application of nontraditional stable-isotope systems to the study of sources and fate of metals in the environment. Environ. Sci. Technol. 42, 655–664. https://doi.org/10.1021/es0870855.

Wen, H., Zhang, Y., Cloquet, C., Zhu, C., Fan, H., Luo, C., 2015. Tracing sources of pollution in soils from the Jinding Pb–Zn mining district in China using cadmium and lead isotopes. Appl. Geochem. 52, 147–154. https://doi.org/10.1016/j.apgeochem.2014.11.025.

Wiederhold, J.G., 2015. Metal stable isotope signatures as tracers in environmental geochemistry. Environ. Sci. Technol. 49, 2606–2624. https://doi.org/10.1021/es504683e.

Wilkinson, J.J., Weiss, D.J., Mason, T.F.D., Coles, B.J., 2005. Zinc Isotope Variation in Hydrothermal Systems: Preliminary Evidence From the Irish Midlands Ore Field. p. 8.

World Health Organization, Food and Agriculture Organization of the United Nations, International Atomic Energy Agency, 1996. Trace Elements in Human Nutrition and Health. World Health Organization, Geneva.

Yanful, E.K., Quigley, R.M., Wayne Nesbitt, H., 1988. Heavy metal migration at a landfill site, Sarnia, Ontario, Canada—2: metal partitioning and geotechnical implications. Appl. Geochem. 3, 623–629. https://doi.org/10.1016/0883-2927(88)90094-7.

Yin, N.-H., Sivry, Y., Benedetti, M.F., Lens, P.N.L., van Hullebusch, E.D., 2016. Application of Zn isotopes in environmental impact assessment of Zn–Pb metallurgical industries: a mini review. Appl. Geochem. 64, 128–135. https://doi.org/10.1016/j.apgeochem.2015.09.016.